

## III-V 族半導體在硫酸蝕刻溶液中之奈米薄膜生成

劉漢忠

大華科技大學機電工程系所

新竹縣芎林鄉大華路 1 號

### 摘要

本研究使用 III-V 族半導體砷化鎵(GaAs)和磷化銦(InP)，測定在光照條件下感應電漿耦合技術的溶解速率和奈米薄膜生成。在這項工作中，使用 X-射線廣角度繞射(WAD)和掠角度繞射(GAD)設備，在室溫下分析 p 型 GaAs 和 InP 的固體氧化物層上的化合物組成。本實驗使用一台 12 千瓦靈敏度極高的旋轉銅陽極型 X 射線源，不僅要分析化學成分，也測量表面氧化物的結構特徵。在  $\text{H}_2\text{SO}_4$  水溶液中，若同時存在  $\text{H}_2\text{O}_2$  氧化劑，研究發現  $\text{GaOOH}$  相會成長於氧化物的表面上，並且使得 GaAs 溶解速率急劇增加。相反地，即使在酸性溶液在光照條件下，InP 和 GaAs 在  $\text{H}_2\text{SO}_4/\text{H}_2\text{O}$  水溶液中之溶解速率會受到嚴格限制，相較於  $\text{H}_2\text{SO}_4/\text{H}_2\text{O}_2/\text{H}_2\text{O}$  溶液，其溶解速率大約小於 3 個數量級的差異，在 GaAs 的表面上也沒有任何  $\text{GaOOH}$  化合物形成。這些反應性質的差異可以解釋在  $\text{H}_2\text{O}_2/\text{H}_2\text{O}$  溶液中，反應是否會在 GaAs 表面上形成  $\text{GaOH}^{2+}$  中間產物的熱力學穩定的能量趨勢，因此 GaAs 的表面上會有  $\text{GaOOH}$  化合物的形成。依據熱力學推測，乃因硫酸溶液中加入  $\text{H}_2\text{O}_2$ ，反應過程會產生  $\text{GaOH}^{2+}$  中間產物，使得 GaAs 在酸液中的反應溶解速率會因此而急遽加速。綜合酸性溶液的蝕刻速率和 X-射線繞射的研究和實驗，可知過氧化氫在硫酸溶液蝕刻 GaAs 的反應中扮演了關鍵的角色。

**關鍵詞：**砷化鎵，磷化銦，感應電漿耦合，奈米薄膜，廣角度繞射，掠角度繞射

## Nanoscale Films of III-V Semiconductor Etched by Sulfuric Acids

HAN-CHUNG LIU

*Department and Institute of Mechatronic Engineering, Ta Hwa University of Science and Technology  
No.1, Dahua Road, QiongLin Shiang, HsinChu County 307, Taiwan*

### ABSTRACT

The dissolution rates and nanoscale films formation of III-V semiconductors GaAs and InP were determined by the inductively coupled plasma technique under illumination. In this work, the compounds of the solid oxide layer on p-type GaAs and InP were identified at room temperature by both X-ray wide angle diffraction (WAD) and glancing angle diffraction (GAD). A 12 kW rotating Cu anode X-ray source ensured high sensitivity, not only to investigate chemical composition, but also to characterize the structural features of the oxides. The GaAs dissolution rate in aqueous  $\text{H}_2\text{SO}_4$  solutions increased dramatically in the presence of  $\text{H}_2\text{O}_2$ , and the  $\text{GaOOH}$  phase was uniquely found

on the oxidized surface. In contrast, the dissolution rate of InP and GaAs in aqueous  $\text{H}_2\text{SO}_4$  was severely restricted even in the most acidic solutions under illumination, about 3-order lower when compared with GaAs in  $\text{H}_2\text{SO}_4/\text{H}_2\text{O}_2/\text{H}_2\text{O}$  solution and no GaOOH compound was formed on the surface of GaAs. The differences in their reactivities can be interpreted in terms of the energetic tendency in the stability of  $\text{GaOH}^{2+}$  intermediate in  $\text{H}_2\text{O}_2$  and in  $\text{H}_2\text{O}$ , which, in turn, determine whether or not the formation of GaOOH on GaAs surface. It is postulated that the production of  $\text{GaOH}^{2+}$  intermediate is thermodynamically favored so that the dissolution rate of GaAs in  $\text{H}_2\text{SO}_4$  system is accelerated by the present of  $\text{H}_2\text{O}_2$ . By combining the etching rate and X-ray diffraction results it is possible to show that  $\text{H}_2\text{O}_2$  play a critical role in the etching of GaAs in  $\text{H}_2\text{SO}_4$  solution.

**Key Words:** GaAs, InP, Inductively coupled plasma, nanoscale films, WAD, GAD

## I · Introduction

Solid-state devices based on III-V compound semiconductor have been developed for using in the metal insulator semiconductor (MIS) systems and optical communications [1~5]. This has created a great deal of interest in the etching and oxidation of these semiconductors, because the resulting surface or interfacial properties evidently affect the characteristics of the devices [6].

X-ray wide angle diffraction (WAD) and glancing angle diffraction (GAD) techniques have been used in this study to establish a much better understanding of the chemical nature of GaAs [7,8] and InP [9~11] surfaces after a variety of chemical treatments. Wet etching and electrochemical oxidation are well-known processes for first removing the native oxide and depositing an insulating layer on these chemically cleaned surfaces. Sulfuric acid is a commonly used solution in substrate preparation for acidic etch. Hydrogen peroxide is a popular choice for the oxidizing component in III-V semiconductor etching and is most commonly paired with  $\text{H}_2\text{SO}_4$ ,  $\text{H}_3\text{PO}_4$ , HCl, or  $\text{NH}_4\text{OH}$ . Therefore,  $\text{H}_2\text{SO}_4$ -based etchants are widely used for many III-V semiconductors [10~12]. The oxidation using  $\text{H}_2\text{SO}_4/\text{H}_2\text{O}$  and optical illumination provides a simple means of growing a thin film on III-V compound. Consequently, sulfuric acid (or  $\text{H}_2\text{SO}_4/\text{H}_2\text{O}_2/\text{H}_2\text{O}$ ) is a frequently used etching solution in substrate preparation.

In the present study, both WAD and GAD techniques were applied to characterize the GaAs and InP surfaces etched in  $\text{H}_2\text{SO}_4/\text{H}_2\text{O}$  and  $\text{H}_2\text{SO}_4/\text{H}_2\text{O}_2/\text{H}_2\text{O}$  solutions under illumination. The GAD technique has several advantages: Ultra

thin films can be investigated, strong signals from such substrates as single crystals can be avoided, and more information can be provided about the preferred orientation of the oxides.

## II · EXPERIMENTAL

The substrate under study was p-type GaAs (100) and InP (100) doped with Zn at a concentration of  $10^{18}$  atom/cm<sup>3</sup>. Two types of etchant were used in this study:  $\text{H}_2\text{SO}_4/\text{H}_2\text{O}$  and  $\text{H}_2\text{SO}_4/\text{H}_2\text{O}_2/\text{H}_2\text{O}$ . All samples were illuminated with a 150 W halogen lamp. The temperature of the test system was maintained at 25 °C. The dissolution rates of GaAs and InP in the solution were measured by inductively coupled plasma (ICP) emission spectrometry. The area of exposed surface to the etchant was 4×5 mm. The constitutional concentration of Ga and In respectively from GaAs and InP as low as 0.1 ppm could be determined.

The compositions of the solid oxide layer on GaAs and InP were identified at room temperature by an MXP 18 XRD meter (Material Analysis and Characterization Co., Japan). The MXP series is an automatic measurement system which employs UNIX as the operation system. Two different XRD analyses were employed in this work: (i) The WAD technique of the conventional  $\theta$ -2 $\theta$  scanning technique, and (ii) the GAD technique of asymmetric-Bragg diffraction. To increase diffraction intensities, a 12 kW rotating Cu anode X-ray source was used. The GAD measurements were performed using a spectrometer attached to the thin-film measuring system. A bent analyzing crystal monochromator used for WAD was

replaced by a flat graphite (0002) for GAD measurements. An incident slit width of 0.1 mm was selected and the thin-film specimen was fixed at one of a range of glancing angles,  $\theta$ , with respect to the incident X-ray beam.

### III · Results and Discussion

The WAD and GAD patterns of the oxidized nanoscale films GaAs surface in  $\text{H}_2\text{SO}_4/\text{H}_2\text{O}_2/\text{H}_2\text{O}$  (1:4:10, volume ratio) etchant are shown in Fig. 1. The intensities of all other oxide peaks are much less 1 % than those from the substrate in WAD (Fig. 1 (a)). The Bragg peaks for the substrate are identified as (200) and (400) reflection planes as shown in Fig. 1 (a). The X-ray diffraction pattern (XRD) of the oxidized surface shows only the sharp peaks which have the normal full width at half maximum (FWHM) [7,8]. The composition of each reaction product was determined by comparing these spacings with the standard X-ray values (JCPDS). Many of the main peaks for each phase were missing because of non-Bragg diffraction conditions.

Figs. 1 (b) and 1 (c) are the result of applying the GAD ( $\theta=1^\circ$  and  $0.5^\circ$ , respectively) technique to the same test sample used in Fig. 1 (a). The multiple peak structures are absent from the GAD, and the peaks occur in completely different positions from those seen in Fig. 1(a). The X-ray penetration depth increases with  $\theta$ , and the differences of GAD peak profiles appear to be due to the differences of GAD with depth. The oxide peaks in Figs. 1 (a), (b) and (c) all exhibit the normal full width at half maximum,<sup>7, 8</sup> suggesting that the oxides are crystalline stoichiometric phases.

Table 1 shows the d-spacings of the oxides grown on the GaAs substrate after etching in 1-18 M  $\text{H}_2\text{SO}_4/\text{H}_2\text{O}$  and in  $\text{H}_2\text{SO}_4/\text{H}_2\text{O}_2/\text{H}_2\text{O}$  (1:4:10) etching system. It can be seen that the results from WAD and GAD indicate the existence of almost the same phases in spite of the drastic decrease in the incident angle of GAD and the resulting decrease in analytical depth. This indicates an adequate compositional uniformity along the growth direction. The XRD pattern showed that other than elemental Ga and As, only the constituent oxides, namely,

gallium oxide ( $\text{Ga}_2\text{O}_3$ ) and arsenic oxides ( $\text{As}_2\text{O}_3$ ,  $\text{H}_5\text{As}_3\text{O}_{10}$ ,  $2\text{As}_2\text{O}_3 \cdot \text{As}_2\text{O}_5 \cdot \text{H}_2\text{O}$ ,  $2\text{H}_3\text{AsO}_4 \cdot \text{H}_2\text{O}$ ) were found on the GaAs surface in  $\text{H}_2\text{SO}_4/\text{H}_2\text{O}$  etches. But in  $\text{H}_2\text{SO}_4/\text{H}_2\text{O}_2/\text{H}_2\text{O}$  etches, in addition to the pattern obtained for the oxides grown in  $\text{H}_2\text{SO}_4/\text{H}_2\text{O}$  etches, a unique phase of GaOOH was detected on the oxidized GaAs surface.

Figs. 2 (a), (b) and (c) show the WAD and GAD patterns, respectively, of the oxidized InP in  $\text{H}_2\text{SO}_4/\text{H}_2\text{O}_2/\text{H}_2\text{O}$  (1:4:10) etchant under illumination. Table 2 lists the d-spacing of InP in 1-18 M  $\text{H}_2\text{SO}_4/\text{H}_2\text{O}$  and  $\text{H}_2\text{SO}_4/\text{H}_2\text{O}_2/\text{H}_2\text{O}$  (1:4:10) etchant systems. A comparison of the diffraction lines obtained by WAD and GAD shows that, the single component oxides,  $\text{In}_2\text{O}_3$  and  $\text{P}_2\text{O}_5$ , as well as mixed component products,  $\text{InPO}_4 \cdot \text{H}_3\text{PO}_4 \cdot 4\text{H}_2\text{O}$ ,  $\text{H}_3\text{PO}_4 \cdot 0.5\text{H}_2\text{O}$ , and  $\text{InPO}_4 \cdot 2\text{H}_3\text{PO}_4 \cdot \text{H}_2\text{O}$ , were observed on the oxidized InP, whether etched in  $\text{H}_2\text{SO}_4/\text{H}_2\text{O}$  or in  $\text{H}_2\text{SO}_4/\text{H}_2\text{O}_2/\text{H}_2\text{O}$ .

The dissolution rates of GaAs in  $\text{H}_2\text{SO}_4/\text{H}_2\text{O}$  and in  $\text{H}_2\text{SO}_4/\text{H}_2\text{O}_2/\text{H}_2\text{O}$  solutions under illumination, determined by ICP, plotted as a function of the etchant concentration, as shown in Fig. 3. Equivalent data are also presented for the dissolution rate of various concentrations from InP. These experiments reveal that a significant difference between the dissolution rates of GaAs in  $\text{H}_2\text{SO}_4/\text{H}_2\text{O}$  and  $\text{H}_2\text{SO}_4/\text{H}_2\text{O}_2/\text{H}_2\text{O}$  etchants is observed. The dissolution rates in  $\text{H}_2\text{SO}_4/\text{H}_2\text{O}$  are much lower and increase only slightly when compared with GaAs in  $\text{H}_2\text{SO}_4/\text{H}_2\text{O}_2/\text{H}_2\text{O}$ . These show that the addition of  $\text{H}_2\text{O}_2$  to  $\text{H}_2\text{SO}_4$  aqueous solution has significant influence on the oxidation process of GaAs. Fig. 3 also shows that the dissolution rates for InP in  $\text{H}_2\text{SO}_4/\text{H}_2\text{O}$  and  $\text{H}_2\text{SO}_4/\text{H}_2\text{O}_2/\text{H}_2\text{O}$  etchants are not discernable and are similar to those of GaAs obtained in  $\text{H}_2\text{SO}_4/\text{H}_2\text{O}$ . It is apparent that the addition of  $\text{H}_2\text{O}_2$  to the aqueous  $\text{H}_2\text{SO}_4$  solution has no significant effect on the InP oxidizing process. On the contrary, the addition of  $\text{H}_2\text{O}_2$  to the aqueous  $\text{H}_2\text{SO}_4$  solution plays an important role in the dissolution of GaAs (Fig. 3).

**Table 1 Chemical compositions for different oxidized GaAs nanoscale films surfaces in H<sub>2</sub>SO<sub>4</sub>/H<sub>2</sub>O and H<sub>2</sub>SO<sub>4</sub>/H<sub>2</sub>O<sub>2</sub>/H<sub>2</sub>O etchants under illumination.**

Etchant	Concentration (M)	Reaction product
H <sub>2</sub> SO <sub>4</sub> /H <sub>2</sub> O	1-18	Ga <sub>2</sub> O <sub>3</sub> , As <sub>2</sub> O <sub>3</sub> , H <sub>5</sub> As <sub>3</sub> O <sub>10</sub> , 2H <sub>3</sub> AsO <sub>4</sub> · H <sub>2</sub> O , Ga , As , 2As <sub>2</sub> O <sub>3</sub> · As <sub>2</sub> O <sub>5</sub> · H <sub>2</sub> O
H <sub>2</sub> SO <sub>4</sub> /H <sub>2</sub> O <sub>2</sub> /H <sub>2</sub> O	1:4:10	Ga <sub>2</sub> O <sub>3</sub> , As <sub>2</sub> O <sub>3</sub> , H <sub>5</sub> As <sub>3</sub> O <sub>10</sub> , 2H <sub>3</sub> AsO <sub>4</sub> · H <sub>2</sub> O , Ga , As , 2As <sub>2</sub> O <sub>3</sub> · As <sub>2</sub> O <sub>5</sub> · H <sub>2</sub> O , GaOOH

**Table 2 Chemical compositions for different oxidized InP nanoscale films surfaces in H<sub>2</sub>SO<sub>4</sub>/H<sub>2</sub>O and H<sub>2</sub>SO<sub>4</sub>/H<sub>2</sub>O<sub>2</sub>/H<sub>2</sub>O etchants under illumination.**

Etchant	Concentration (M)	Reaction product
H <sub>2</sub> SO <sub>4</sub> /H <sub>2</sub> O	1-18	InPO <sub>4</sub> · H <sub>3</sub> PO <sub>4</sub> · 4H <sub>2</sub> O , H <sub>3</sub> PO <sub>4</sub> · 0.5H <sub>2</sub> O ,
H <sub>2</sub> SO <sub>4</sub> /H <sub>2</sub> O <sub>2</sub> /H <sub>2</sub> O	1:4:10	InPO <sub>4</sub> · 2H <sub>3</sub> PO <sub>4</sub> · H <sub>2</sub> O , In <sub>2</sub> O <sub>3</sub> , P <sub>2</sub> O <sub>5</sub>

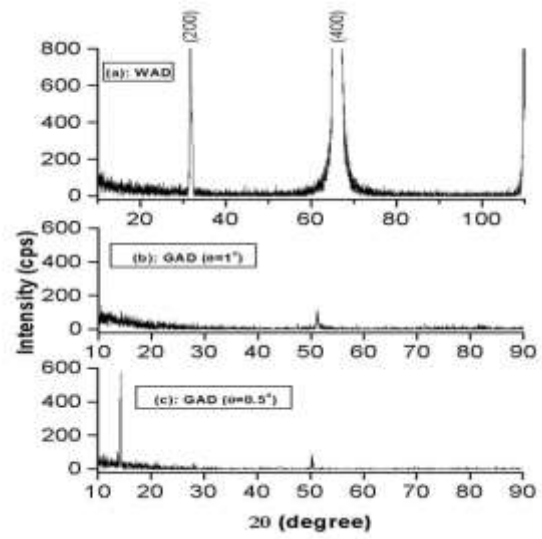


**Figure 1 (a) WAD of oxide on the surface of p-GaAs (100) in H<sub>2</sub>SO<sub>4</sub>/H<sub>2</sub>O<sub>2</sub>/H<sub>2</sub>O (1:4:10) etchant under illumination. (b) GAD (θ= 1°) and (c) GAD (θ= 0.5°) of oxide on the surface of p-GaAs (100) in H<sub>2</sub>SO<sub>4</sub>/H<sub>2</sub>O<sub>2</sub>/H<sub>2</sub>O (1:4:10) etchant under illumination.**

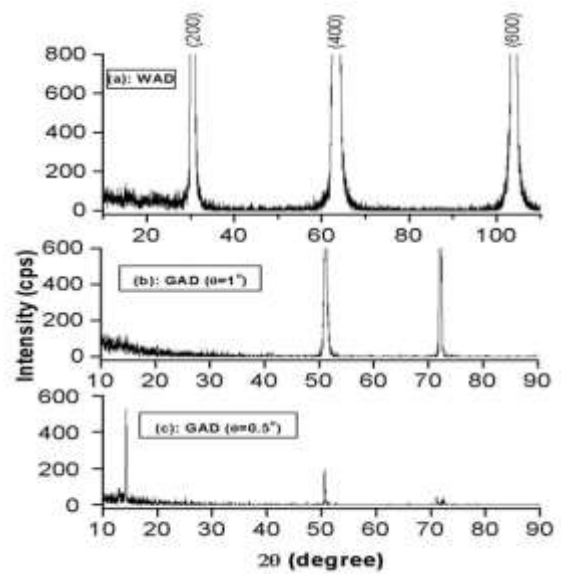


**Figure 2 (a) WAD of oxide on the surface of p-InP (100) in H<sub>2</sub>SO<sub>4</sub>/H<sub>2</sub>O<sub>2</sub>/H<sub>2</sub>O (1:4:10) etchant under illumination. (b) GAD (θ= 1°) and (c) GAD (θ= 0.5°) of oxide on the surface of p-InP (100) in H<sub>2</sub>SO<sub>4</sub>/H<sub>2</sub>O<sub>2</sub>/H<sub>2</sub>O (1:4:10) etchant under illumination.**

## IV、Conclusions

(1) The result of ICP emission spectrometry showed that the reaction rate of the illuminated p-type GaAs and InP compound semiconductors in  $\text{H}_2\text{SO}_4/\text{H}_2\text{O}$  etchant without the effect of  $\text{H}_2\text{O}_2$  occurred very slowly. In contrast, the GaAs specimen in  $\text{H}_2\text{SO}_4/\text{H}_2\text{O}_2/\text{H}_2\text{O}$  system is more than 1000-fold increase of the dissolution rate when comparing with InP in the same etching system of  $\text{H}_2\text{SO}_4/\text{H}_2\text{O}_2/\text{H}_2\text{O}$ .

(2) The XRD pattern showed that other than elemental Ga and As, only their constituent oxides,  $\text{Ga}_2\text{O}_3$ ,  $\text{As}_2\text{O}_3$ ,  $\text{H}_5\text{As}_3\text{O}_{10}$ ,  $2\text{As}_2\text{O}_3 \cdot \text{As}_2\text{O}_5 \cdot \text{H}_2\text{O}$ , and  $2\text{H}_3\text{AsO}_4 \cdot \text{H}_2\text{O}$  were found on the GaAs surface in  $\text{H}_2\text{SO}_4/\text{H}_2\text{O}$  etches. But in  $\text{H}_2\text{SO}_4/\text{H}_2\text{O}_2/\text{H}_2\text{O}$  etches, in addition to the diffraction pattern obtained for oxides grown in  $\text{H}_2\text{SO}_4/\text{H}_2\text{O}$  etches,  $\text{GaOOH}$  was detected as the extra phase on GaAs surface. In contrast, no  $\text{InOOH}$  compound was observed on the InP surface in both etching systems. Thus,  $\text{H}_2\text{O}_2$  does not play any essential role in the dissolution of InP.

## References

1. H. H. Wieder, J. Vac. Sci. Technol., A2, 97 (1984).
2. C. W. Wilmsen, L. G. Meiners, and D. A. Collins, Thin Solid Films, 46, 331 (1977).
3. H. Terao, T. Ito, and Y. Saki, Electr. Eng. Jpn., 94, 127 (1974).
4. D. A. Baglee, D. K. Ferry, C. W. Wilmsen, and H. H. Wieder, J. Vac. Sci. Technol., 17, 1032 (1980).
5. T. Ikoma and H. Yokomizo, IEEE Trans. Electron Devices, ED-23, 521 (1976).
6. S. M. Spitzer, B. Schwartz, and M. Kuhn, J. Electrochem. Soc., 120, 669 (1973).
7. H. F. Hsieh and H. C. Shih, J. Electrochem. Soc., 138, 1965 (1991).
8. H. C. Liu and H. C. Shih, (unpublished).
9. H. F. Hsieh and H. C. Shih, J. Appl. Phys., 66, 3542 (1989).
10. H. F. Hsieh and H. C. Shih, J. Electrochem. Soc., 137, 1348 (1990).
11. H. F. Hsieh and H. C. Shih, J. Electrochem. Soc., 138, 1304 (1991).
12. S. Adachi and H. Kawaguchi, J. Electrochem. Soc., 128, 1342 (1981).